Tuba stimulates intracellular N-WASP-dependent actin assembly

Eva M. Kovacs[1], Robert S. Makar[1,2] and Frank B. Gertler[1,*]

[1]Department of Biology, Massachusetts Institute of Technology, Cambridge, MA 02139, USA
[2]Department of Pathology, Massachusetts General Hospital, Boston, MA 02114, USA
*Author for correspondence (e-mail: fgertler@mit.edu)

Accepted 3 April 2006
Journal of Cell Science 119, 2715-2726 Published by The Company of Biologists 2006
doi:10.1242/jcs.03005

Summary

Tuba is a multidomain scaffolding protein that links cytoskeletal dynamics and membrane trafficking pathways. The N-terminus of Tuba binds dynamin1, and the C-terminus contains domains that can interact with signaling pathways and cytoskeletal regulatory elements. We investigated Tuba localization, distribution and function in B16 melanoma cells. Tuba overexpression stimulated dorsal ruffles that occurred independently of dynamin function. Tuba expression induced actin-driven motility of small puncta that required the C-terminal SH3, GEF and BAR domains. Additionally, Tuba was recruited to lipid vesicles generated by overexpression of phosphatidylinositol-4-phosphate 5-kinase type Iα (PIP5Kα), localizing prominently to the head of the comets and at lower levels along the actin tail. We propose that Tuba facilitates dorsal ruffling of melanoma cells through direct interaction with actin-regulatory proteins and the recruitment of signaling molecules to lipid microdomains for the coordinated assembly of a cytoskeletal network. Knockdown of Tuba by RNA interference (RNAi) attenuated PIP5Kα-generated comet formation and the invasive behavior of B16 cells, implying that Tuba function is required for certain aspects of these processes. These results suggest first that Tuba-stimulated dorsal ruffling might represent a novel mechanism for the coordination of N-WASP-dependent cytoskeletal rearrangements and second that Tuba function is implicated in motility processes.

Supplementary material available online at
http://jcs.biologists.org/cgi/content/full/119/13/2715/DC1

Key words: N-WASP, Tuba, Invasion, Cytoskeleton

Introduction

Rearrangement of the cytoskeleton is tightly regulated by multiple signaling pathways. Members of the Wiskott-Aldrich syndrome protein (WASP) family are major regulators of de novo actin nucleation from the Arp2/3 complex (Higgs and Pollard, 2001). N-WASP is a ubiquitous member of this family and is activated in vitro by a variety of signaling molecules including phosphatidylinositol (4,5)-bisphosphate [PtdIns(4,5)P_2], Cdc42 and WASP-interacting protein (WIP) (Moreau et al., 2000; Prehoda et al., 2000; Rohatgi et al., 2000). N-WASP activity is regulated by an intramolecular interaction that is alleviated following concomitant binding of Cdc42-GTP to the Cdc42/Rac interactive binding (CRIB) domain and PtdIns(4,5)P_2 to the polybasic region (Higgs and Pollard, 2000; Kim et al., 2000). Several other proteins have been shown to interact with N-WASP and regulate its activity, including cortactin (Kempiak et al., 2005; Weaver et al., 2002), Nck (Benesch et al., 2002), Grb2 (Carlier et al., 2000), WISH (Fukuoka et al., 2001) and Toca-1 (Ho et al., 2004). Activated N-WASP can interact directly with the Arp2/3 complex to stimulate actin nucleation (Machesky and Insall, 1998; Rohatgi et al., 1999).

N-WASP-stimulated actin assembly is responsible for events as diverse as membrane ruffling (Zalevsky et al., 2001), endocytosis (Kessels and Qualmann, 2002) and the propulsion of intracellular vesicles (Benesch et al., 2002; Rozelle et al., 2000). All of these processes require spatial targeting of protein complexes through interactions with PtdIns(4,5)P_2-rich lipid microdomains. Subcellular concentrations of PtdIns(4,5)P_2 are regulated through the actions of phosphatidylinositol phosphate kinases (PIPKs) (Oude Weernink et al., 2004), with type Iα PIPKs being the predominant isoform in platelet-derived growth factor (PDGF)-stimulated, Rac-dependent membrane ruffles (Doughman et al., 2003). It has been proposed that scaffolding proteins can influence cell migration through direct regulation of the enzymatic activity of PIPKs and interaction with GTPases, as is observed for the LIM protein Ajuba (Kisseleva et al., 2005).

Tuba is a multidomain scaffolding protein that is ubiquitously expressed and consists of four N-terminal SH3 domains that bind directly to dynamin1, an internal BAR (for 'Bin, Amphiphysin, Rvs') domain, a GTPase exchange factor (GEF) domain specific for the Rho-family GTPase Cdc42, and two C-terminal Src-homology 3 (SH3) domains. The extreme C-terminal SH3 domain binds multiple actin-regulatory proteins directly, including N-WASP and Ena/vasodilator stimulated phosphoprotein (Ena/VASP) (Salazar et al., 2003). The structural complexity highlights the potential for Tuba to integrate signaling and trafficking pathways with cytoskeletal rearrangement events.

Given that (1) the C-terminal SH3 domain of Tuba can bind directly to N-WASP, (2) Tuba is a GEF specific for Cdc42, and

(3) BAR domains can sense and/or induce membrane curvature, we examined the role of Tuba in the assembly of cytoskeletal networks involved in intracellular movement and membrane protrusive events. To accomplish this, we focused on a splice variant of Tuba (mini-Tuba, mTuba), lacking the four N-terminal dynamin-binding SH3 domains. mTuba is typically expressed in the same tissues and cell lines that express full-length Tuba (Salazar et al., 2003) (data not shown). Moreover, manipulation of mTuba affords analysis of Tuba function independent of its interaction with dynamin.

Membrane ruffling is often a result of growth factor stimulation and is recognized as a signal for the transition of a cell to a more motile state (Jiang, 1995). Here, we describe stimulation of dorsal ruffling that results from the overexpression of mTuba and occurs in the absence of growth factors. These membrane protrusions are distinct in nature from the conventional circular dorsal waves observed following growth factor stimulation (Dowrick et al., 1993; Mellstrom et al., 1988), and occur randomly and sporadically across the whole cell. We show that core components of the N-WASP-associated complex responsible for actin nucleation in various cellular events were observed to localize to mTuba puncta and N-WASP activity was essential for puncta localization.

We propose that mTuba acts as a scaffold for the assembly of molecular machinery required for N-WASP-dependent cytoskeletal rearrangements. We demonstrate that knockdown of Tuba function perturbs PIP5Kα-generated comet formation and retards cellular invasion, and we speculate that Tuba function might be required for these processes.

Results

mTuba overexpression stimulates actin-dependent membrane ruffling in the absence of growth factors

B16-F1 low-metastatic murine melanoma cells form large, flat lamellipodia and display membrane ruffling activity; therefore, we chose to examine the distribution of mTuba in these cells. A low level of dorsal ruffling is observed in B16-F1 cells, but sevenfold overexpression of GFP-mTuba (Fig. 1B) significantly stimulated the formation of transient dorsal ruffles. In control cells co-transfected with green fluorescent protein (GFP) plus monomeric red fluorescent protein (mRFP)-actin, 0.2±0.1 ruffles formed per minute (n=4, 10 minute experiment); by contrast, overexpression of GFP-mTuba with mRFP-actin stimulated the formation of 1.0±0.5 ruffles/minute (n=6, 10 minute experiment). The ruffles were easily detectable by actin fluorescence and radiated concentrically outwards with no apparent polarization, even traversing the plasma membrane over the nucleus (Fig. 1C).

mTuba localizes to puncta at the trailing edge of ruffles

mTuba concentrated in puncta that were juxtaposed to the cell body at the base of the ruffle, as shown by overlay of time-lapse images of GFP-mTuba and mRFP-actin (Fig. 1E and Movie 1, supplementary material). The puncta initially coalesced and, as the ruffle evolved, the movement of the puncta resembled a broad wave front that remained associated with the trailing edge as the ruffle progressed. The actin network that constituted the framework of the ruffle appeared to be ahead of the puncta as the ruffle developed and expanded. Formation of puncta was not an artifact of GFP expression because co-expression of a GFP control vector with Cherry-mTuba, constructed by replacing the GFP fluorophore in GFP-mTuba with a Cherry fluorophore (see Materials and Methods), resulted in puncta formation only for Cherry-mTuba (Fig. 1D).

Table 1. Summary of co-localization of constituents with mTuba in B16-F1 melanoma cells by immunofluorescence or time-lapse video microscopy

Constituent	Assay	Localization
N-WASP	IF	Robust co-localization at mTuba puncta
Arp3	TL	Robust co-localization at mTuba puncta
WIP	TL	Robust co-localization at mTuba puncta
Toca-1	TL	Robust co-localization at mTuba puncta
Tuba 1 (full length)	TL	Robust co-localization at mTuba puncta
WtCdc42	TL	Co-localization at mTuba puncta
N17Cdc42	TL	Increased formation of mTuba puncta
N17Rac1	IF	No obvious change in mTuba puncta localization
Cortactin	IF	Subpopulation of mTuba puncta
PIP5KIα-generated vesicles	IF	mTuba localization to head of comets
Evl	TL	Localized to leading edge of ruffle No apparent co-localization with mTuba puncta
VASP	IF	Localized to leading edge of ruffle No apparent co-localization with mTuba puncta
Texas Red-Dextran	IF	Bright circumferential localization of mTuba (subpopulation distinct from mTuba puncta)
Caveolin 1	IF	Subpopulation of mTuba
Huddy 2 (dynamin1)	IF	Subpopulation of mTuba
Texas Red-Transferrin	IF	No inhibition of transferrin uptake
GM130	IF	No apparent co-localization

IF, immunofluorescence: fixed B16s were immunostained for Tuba (affinity-purified pAb) and the constituent stated.
TL, time-lapse imaging: B16s were transfected using Amaxa with appropriate constructs.

Multiple analyses were performed in an attempt to identify constituents associated with Tuba puncta and these are documented in Table 1 in order of decreasing, apparent co-localization. No obvious co-localization was observed with Golgi markers, Caveolin 1 or dynamin using an affinity-purified anti-Tuba antibody (Salazar et al., 2003). Bright Tuba staining was observed around TR-dextran vacuoles, suggesting that Tuba might function in macropinocytosis in addition to the puncta associated with ruffling.

mTuba has limited co-localization with actin at puncta

To determine the extent of association of mTuba with actin in ruffles, we measured the amount of overlap of the two fluorophores over time (see Materials and Methods). Analysis of the mTuba puncta and actin content at ruffles demonstrated that, on average, 10-20% of the total area of mTuba puncta and actin signals overlapped at any particular time (Fig. 1F). This limited overlap is supported by the observation that overlay of mTuba and actin images showed that puncta localized to the trailing edge of the actin network that constituted the body of the ruffle, but did not appear to reside within the ruffle per se (Fig. 1E, merged images).

We analyzed the behavior of mTuba puncta in ruffles over time using kymographic analysis to create a cross-sectional view of pixel intensities in a defined region of a stack of time-lapse images. As the resultant image represents movement in

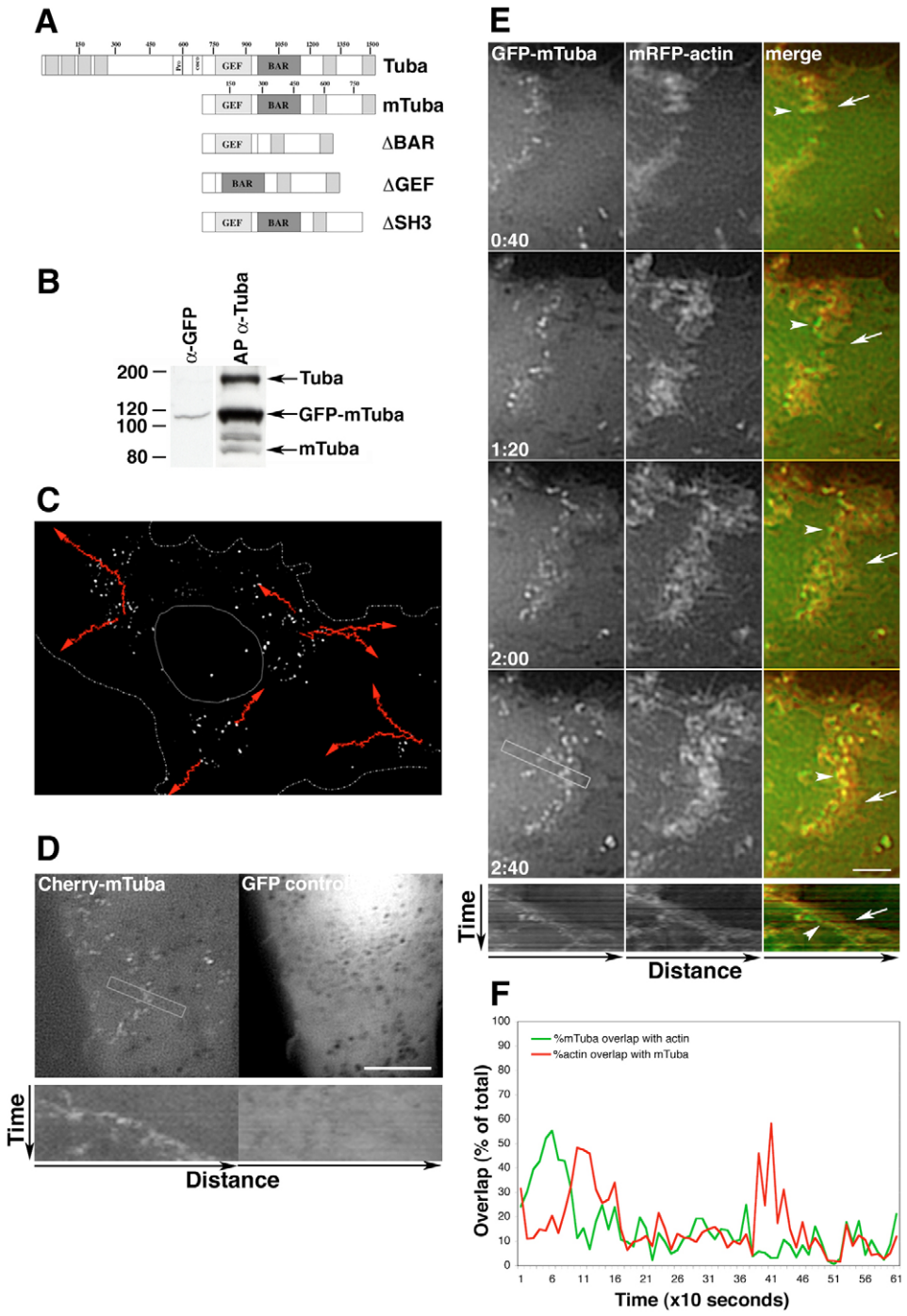

Fig. 1. mTuba overexpression stimulates dorsal ruffling. (A) Tuba isoforms. Domain structure of full-length Tuba (Tuba) and mini-Tuba (mTuba) are indicated. Tuba possesses four tandem N-terminal SH3 domains (gray boxes), which bind directly to dynamin. The C-terminal SH3 domain binds N-WASP. Schematic representations of mTuba mutants are indicated. (B) Overexpression of GFP-mTuba. B16 cells were transfected with GFP-mTuba and cell lysates were probed for GFP and Tuba using anti-GFP antibody (α-GFP) and affinity-purified anti-Tuba antibody (AP α-Tuba), respectively. (C) GFP-mTuba expression wave front tracking. The front of GFP-mTuba puncta was tracked through 30 frames of a time-lapse movie and shows apparent random movement. (D) A single image from a time-lapse movie of B16 cells co-transfected with Cherry-mTuba and GFP. The lower panel represents kymographs constructed from the boxed region from each image. Note movement of mTuba puncta but not GFP. (E) Series of time-lapse images of a B16-F1 cell co-transfected with GFP-mTuba and mRFP-actin (Movie 1, supplementary material). Tuba puncta localize to the trailing edge of the actin ruffle and radiate outwards concomitant with the passage of the ruffle. The rectangle indicates the region of the movie used to generate the kymographs. Average speed of ruffles is 1.32±0.38 microns/minute (n=29). Arrows indicate the leading edge of the ruffle. Arrowheads indicate localization of mTuba puncta to the trailing edge of the ruffle. (F) Percentage of total area of Tuba (green) and actin (red) from (E) that overlap during ruffle formation over time (see Materials and Methods). Plot indicates that approximately 10% of the total Tuba population overlaps actin directly, and that approximately 10% of the actin population overlaps Tuba puncta directly. Bars: D, 5 μm; E, 3 μm.

time, kymographic analysis of puncta fluorescence in each frame of a time-lapse movie (Movie 1, supplementary material) enabled calculation of the speed puncta moved across the surface of the cell. A line, seven pixels in width, was drawn from the region of initial puncta formation to the end point of puncta transition (represented by the box in Fig. 1E). Grayscale intensity values for pixels within this region were plotted for each frame of the movie, such that the values from the first frame are represented in the first row of the kymograph, and the values from the second frame are represented in the second row, etc. The fluorescence in the kymograph represents the movement of the puncta with time and the slope of the path of detected fluorescence represents the speed of transition across the surface of the cell. These kymographs do not describe leading-edge dynamics of the ruffle itself. mTuba puncta progressed across the cell at an average speed of 1.32±0.38 microns/minute (n=29, 5 cells) with a maximum speed of 1.87 microns/minute and a minimum speed of 0.78 microns/minute (Fig. 1E, lower panel). GFP-mTuba puncta seem to remain associated with ruffles such that movement of the puncta correlates with the relative movement of the ruffle. Analysis was performed simultaneously on corresponding images for fluorescence of mRFP-actin (Fig. 1E, right lower panel).

Domains required for mTuba-dependent ruffling

To determine the requirement for the major domains within mTuba for puncta motility and dorsal ruffling, we constructed mutants in which these domains were deleted, and examined their effect on ruffle formation. The C-terminal SH3 domain of mTuba is known to interact with actin-regulatory proteins including members of the Ena/VASP and WASP family of actin regulators (Salazar et al., 2003). When overexpressed, an mTuba mutant lacking this SH3 domain (Cherry-ΔSH3, Fig. 1A) localized diffusely throughout the cytoplasm and no excess ruffling was observed (Fig. 2A). This indicates that the C-terminal SH3 domain of mTuba is required for puncta formation.

Tuba is a GEF with specificity for the Cdc42 Rho-family GTPase (Salazar et al., 2003). An mTuba mutant that is incapable of activating Cdc42 directly (Cherry-ΔGEF, Fig. 1A) formed puncta that were associated with actin as indicated by kymography, but did not stimulate ruffle formation (Fig. 2B and lower panel), suggesting that activation of Cdc42 by mTuba is necessary to stimulate actin assembly for ruffle formation.

BAR-domain-containing proteins are recognized for their ability to bind preferentially to highly curved, negatively charged membranes and, under certain conditions, these domains are capable of inducing membrane curvature (Farsad et al., 2001). A ΔBAR mTuba mutant (Cherry-ΔBAR) neither formed puncta nor induced the formation of dorsal ruffles (Fig. 1A, Fig. 2C). However, the transfected cells displayed excessive peripheral ruffling, as indicated by kymography, at which mTuba and actin co-localized. This suggests that a functional BAR domain is required for mTuba-stimulated dorsal ruffling.

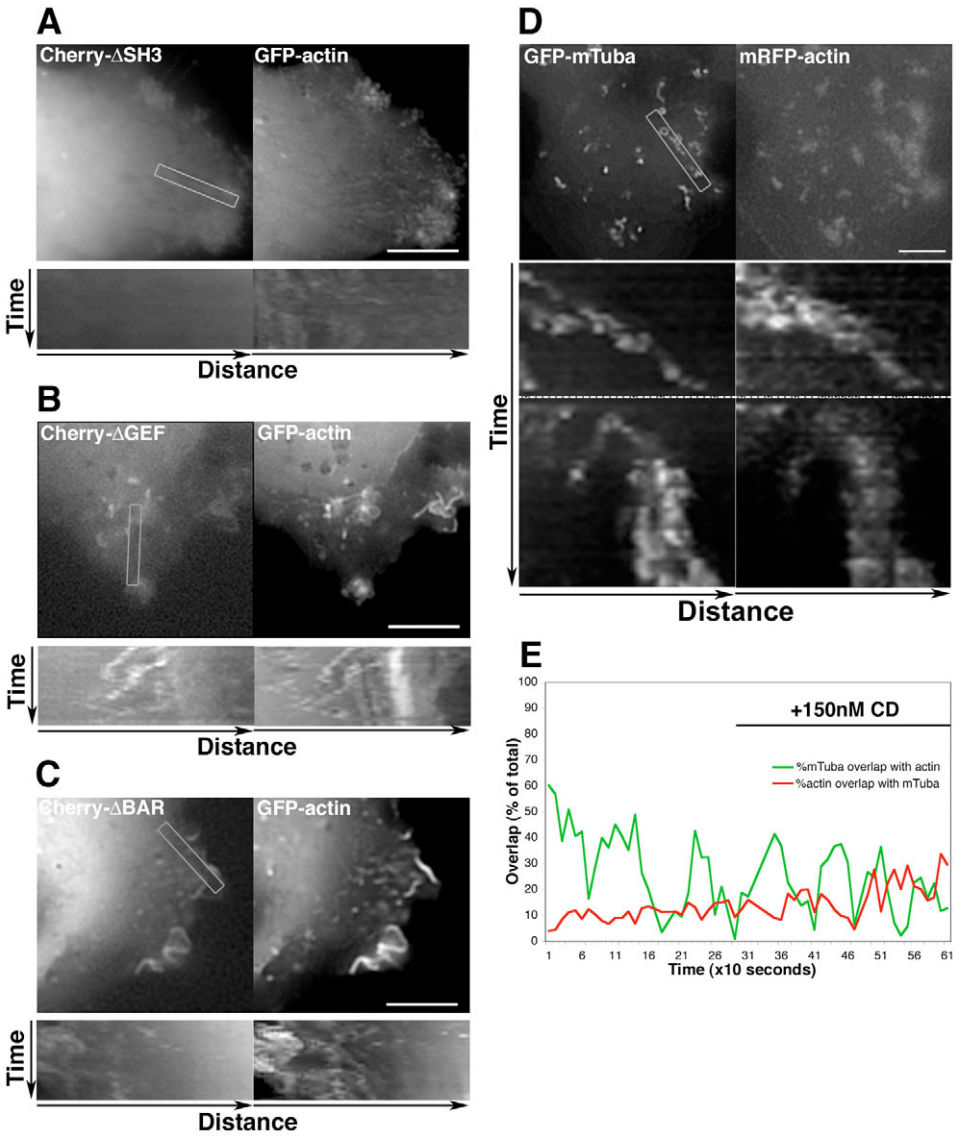

Fig. 2. Inhibition of actin polymerization and deletion of mTuba domains disrupts dorsal ruffle formation. (A) Co-expression of Cherry-ΔSH3 and GFP-actin in B16 cells. Deletion of the actin-regulatory protein-binding domain of mTuba results in cytoplasmic distribution of mTuba with no visible puncta formation. Actin organization is also disrupted. Box indicates region of movie used to generate kymographs. Kymographs confirm cytoplasmic distribution of the mutant. (B) Co-expression of Cherry-ΔGEF and GFP-actin in B16 cells. Deletion of the GEF domain of mTuba results in puncta formation but no ruffling. Box indicates region of movie used to generate kymographs. Kymographs show near-stationary puncta. (C) Co-expression of Cherry-ΔBAR and GFP-actin in B16 cells. Deletion of the BAR domain of mTuba causes extensive peripheral ruffling but no dorsal ruffling. Box indicates region of movie used to generate kymographs. Kymographs show rapid peripheral ruffling activity. (D) B16-F1 cells co-transfected with GFP-mTuba and mRFP-actin and treated with 50 nM cytochalasin D (CD). Image shown is following CD treatment. Boxed area indicates region used to generate kymographs. Average speed of puncta following CD treatment is 0.03±0.19 microns/minute (n=6). Actin polymerization is inhibited, but mTuba remains associated with the actin cytoskeleton at 'patches'. Kymographs are derived from the full movie with CD addition at five minutes. Dotted line indicates time of CD addition. Note that, following CD treatment, mTuba puncta fail to move. (E) Percentage of total area of mTuba (green) and actin (red) that coexist during ruffle formation in (D) (see Materials and Methods). Plots show that the percentage of actin overlapping with mTuba puncta increases following CD treatment at actin 'patches'. Bars, 5 μm.

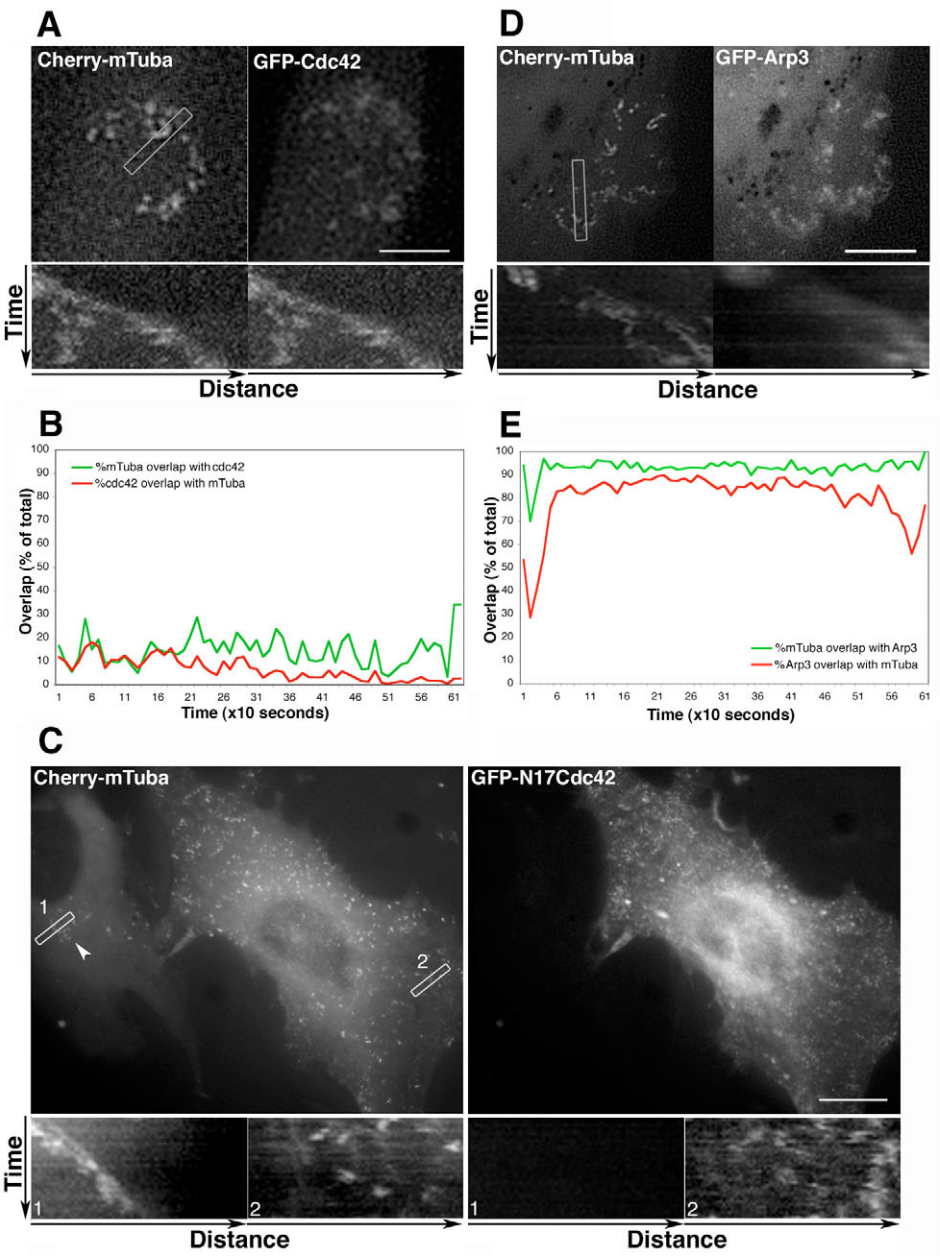

Fig. 3. Cdc42 and Arp3 localize to mTuba-stimulated dorsal ruffles. (A) A single frame taken from a 10 minute movie of B16 cells co-transfected with Cherry-mTuba and GFP-Cdc42 shows co-localization of mTuba and Cdc42 at puncta. Box indicates region of movie used for kymograph construction. Average speed of puncta is 1.52±0.34 microns/minute (n=5). (B) Percentage of total area of mTuba (green) and Cdc42 (red) that coexist during ruffle formation in A. 10% of mTuba co-localizes with Cdc42, and 5-10% of the population of Cdc42 co-localizes with mTuba. (C) B16 cells were co-transfected with Cherry-mTuba and GFP-N17Cdc42. N17Cdc42 generates greater numbers of mTuba puncta relative to cells transfected with Cherry-mTuba alone (arrow indicates formation of ruffle). Boxes indicate regions of movie used for kymograph construction. Note limited mobility of mTuba puncta when co-expressed with GFP-N17Cdc42. (D) A single frame taken from a movie of B16 cells co-transfected with Cherry-mTuba and GFP-Arp3 shows co-localization of Arp2/3 and mTuba at puncta. Box indicates region of movie used for kymograph construction. Speed of puncta is 1.01±0.15 microns/minute (n=6). (E) Percentage of total area of mTuba (green) and Arp3 (red) that coexist during ruffle formation in (D). Approximately 90% of mTuba co-localizes with Arp3, and ~85% of the population of Arp3 co-localizes with mTuba. Bars: A,D, 5 μm; C, 15 μm.

Actin polymerization is required for mTuba-induced ruffle formation

As only a minority of the population of mTuba puncta was associated with actin, we wanted to confirm dependence on actin polymerization for mTuba-stimulated ruffle formation. B16 cells co-expressing GFP-mTuba and mRFP-actin were treated with 5 0 nM cytochalasin D (CD), a concentration that blocks free barbed ends inhibiting elongation of actin filaments (Bear et al., 2002; Cooper, 1987; Sampath and Pollard, 1991). Cessation of ruffling was observed when actin assembly was inhibited (Fig. 2D). However, whereas mTuba puncta remained associated with the cytoskeleton for the duration of the experiment, they became immobile with little or no turnover (Fig. 2D, kymograph; speed=0.03±0.19 microns/minute). In fact, the amount of co-localization between mTuba and actin increased with continued exposure to drug (20-30% versus 10-20% for untreated cells; Fig. 2E, Fig. 1F), suggesting that recruitment of components to a predetermined site occurred in the absence of actin polymerization.

Cdc42 and Arp2/3 localize to mTuba puncta during ruffle formation

We determined through mutational analysis that the ability of mTuba to bind actin-regulatory proteins and activate signal cascades was essential for ruffle formation. As deletion of the Cdc42-specific GEF domain within mTuba prevented ruffle formation, we sought to demonstrate the involvement of Cdc42 (Fig. 3A). Kymography showed that the GTPase moved with mTuba as the ruffle progressed (Fig. 3A, lower panel; speed=1.52±0.34 microns/minute, n=5), but only low levels of Cdc42 were observed to co-localize with mTuba (<10%, Fig. 3B). These levels decreased with time, concomitant with

expiration of the ruffle, suggesting that the GTPase is recruited to the ruffle by mTuba, where it is activated. Interestingly, overexpression of a dominant-negative form of Cdc42 (N17) resulted in greater numbers of mTuba puncta with limited irregular motility (Fig. 3C and lower panel), supporting a requirement for GTPase activation for the productive formation of mTuba-stimulated dorsal ruffles. Of note, overexpression of dominant-negative Rac (N17) did not appear to affect mTuba puncta (Table 1), but did increase recruitment of mTuba to peripheral ruffles (data not shown).

When activated, the multiprotein Arp2/3 complex assembles branched networks of actin filaments that constitute the cytoskeletal arrangement documented for ruffles and lamellipodia (Svitkina and Borisy, 1999; Zalevsky et al., 2001). Arp3 co-localized with mTuba puncta in ruffles (Fig. 3D). Quantitation showed that the majority of the Arp2/3 complex observed during ruffling was associated with mTuba (80% Arp3 and 90% mTuba; Fig. 3E) and that the complex moved as the ruffle advanced (Fig. 3E, kymograph; speed=1.01±0.15 microns/minute, n=6). The overlap between mTuba and Arp3 decreased with expiration of the ruffle.

Evl localizes to the leading edge of mTuba-induced dorsal ruffles

Tuba was identified as an Ena/VASP interactor (Salazar et al., 2003) and deletion of the SH3 domain of mTuba that mediates this interaction inhibited formation of mTuba puncta and subsequent ruffling (this work). Interestingly, however, co-expression of mRFP-Evl and GFP-mTuba showed that Evl was not associated with mTuba puncta, but localized to the leading edge of the dorsal ruffles (Fig. 4A) with a similar localization pattern observed for VASP (Table 1). Targeting of the C-terminal SH3 domain of Tuba to mitochondria did not sequester Evl from the leading edge or focal adhesions (data not shown). Additionally, co-expression of Cherry-mTuba with GFP-FPPPP-mito, which sequesters Ena/VASP proteins and is known to phenocopy Ena/VASP loss of function (Bear et al., 2000), did not inhibit mTuba-stimulated ruffling (Table 2). Collectively, these results suggest that Ena/VASP proteins are not directly involved with the regulation of mTuba function in dorsal ruffles.

N-WASP, WIP, Toca-1 and cortactin co-localize with mTuba at puncta

N-WASP and Tuba are direct binding partners, mediated by the C-terminal SH3 domain of Tuba (Salazar et al., 2003). Since Ena/VASP proteins did not appear to be required for mTuba-induced ruffle formation, we investigated the requirement of N-WASP for this process. We first examined the localization of N-WASP in cells transfected with mTuba. As shown in Fig. 4B, robust co-localization between mTuba and N-WASP at puncta is observed, suggesting that this interaction may be central to the formation of dorsal ruffles.

N-WASP exists cytoplasmically in an autoinhibited state and a set of molecules drives its activation (Higgs and Pollard, 2000; Kim et al., 2000). Also, the WASP-interacting protein (WIP) is implicated in the spatial control of actin assembly through N-WASP (Moreau et al., 2000) and, more recently, Toca-1 has been described as necessary for N-WASP activation through Cdc42 in *Xenopus* oocyte extracts (Ho et al., 2004). We observed co-localization of WIP and mTuba (Fig. 4C) as well as co-localization of mTuba and Toca-1 (Fig. 4D) at puncta. These results suggest that WIP and Toca-1 might be required for regulation of mTuba-stimulated actin assembly through N-WASP.

In addition, cortactin binds directly to N-WASP and is involved in its activation and the subsequent stimulation of actin assembly through Arp2/3 (Kempiak et al., 2005).

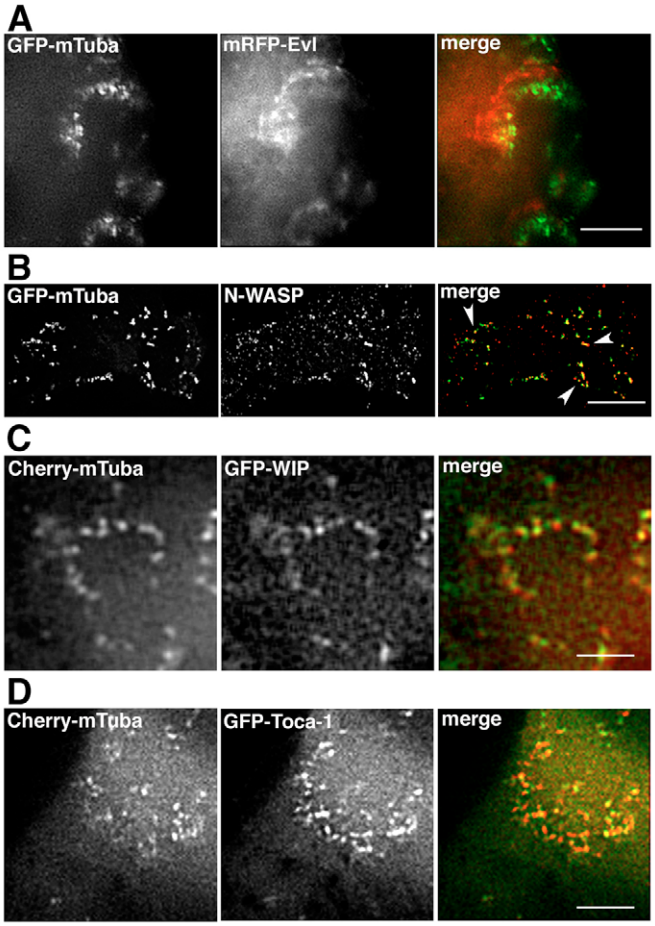

Fig. 4. mTuba co-localizes with N-WASP, WIP and Toca-1, but not Evl at puncta. (A) B16 cells were co-transfected with GFP-mTuba and mRFP-Evl. Evl localized in discrete bands at the leading edge, distinct from puncta, in mTuba-stimulated dorsal ruffles. (B) B16 cells transfected with GFP-mTuba were cultured on glass coverslips, fixed and stained for N-WASP. Arrowheads indicate robust mTuba and N-WASP co-localization at puncta. (C,D) B16 cells were co-transfected with Cherry-mTuba and either (C) GFP-WIP or (D) GFP-Toca-1. Merged images depict co-localization of mTuba with WIP and Toca-1. Bars: A,C, 3 μm; D, 5 μm; B, 15 μm.

Table 2. Summary of effects of agents on mTuba-stimulated ruffle formation in B16-F1 melanoma cells observed by time-lapse video microscopy

Agent	Effect
FPPPP-mito	No inhibition of ruffling (co-expressed with Cherry-mTuba)
Wortmannin	No inhibition of ruffling (30 minutes)
RNAi 'A'	Limited dorsal ruffling (10 minute observation), but not peripheral ruffling
RNAi 'B'	Inhibition of dorsal ruffling (10 minute observation), but not peripheral ruffling

Cortactin was observed to co-localize with N-WASP and mTuba at a limited number of puncta (Table 1), suggesting that cortactin function might not be essential for ruffle formation.

N-WASP activity is essential for mTuba-induced puncta formation and motility

To determine the requirement of N-WASP for Tuba function, we specifically inhibited N-WASP with a small molecule inhibitor, wiskostatin, which is thought to act by maintaining N-WASP in an autoinhibited conformation. At a concentration of 10 μM, wiskostatin specifically inhibits N-WASP without directly affecting actin (Peterson et al., 2004). Treatment of cells expressing GFP-mTuba with 10 μM wiskostatin resulted in the dissolution of mTuba puncta and a cessation of ruffling (Fig. 5A). Quantitation of the intensity of mTuba puncta over time showed that wiskostatin inhibition of N-WASP caused mTuba puncta to disappear within 8 minutes (n=3 cells), with the population of mTuba puncta reduced to 50% 3 minutes following treatment (Fig. 5B). Total dissolution of puncta suggests that N-WASP activity is essential for mTuba function in dorsal ruffles. These results, combined with the observations that (1) Ena/VASP proteins did not localize to mTuba puncta and (2) deletion of the C-terminal SH3 domain of mTuba altered the cellular localization of mTuba, indicate that mTuba specifically requires direct interaction with active N-WASP in an active conformation to stimulate actin assembly for dorsal ruffling.

mTuba localizes to type I PIP5Kα-induced vesicles

PtdIns(4,5)P_2 is important in the regulation and establishment of lipid microdomains that provide a platform for the coordination of signaling cascades, actin assembly and membrane protrusion (Honda et al., 1999; Raucher et al., 2000). Thus, localized accumulation of PtdIns(4,5)P_2 might serve to mark sites for cellular protrusion through N-WASP sensing of lipid microdomains (Papayannopoulos et al., 2005) in conjunction with stimulation of N-WASP activity (Higgs and Pollard, 2000; Kim et al., 2000). PtdIns(4,5)P_2 is synthesized by phosphoinositide 3-kinase (PI 3-kinase) and treatment with the fungal toxin wortmannin blocks this pathway. To determine whether PI 3-kinase was implicated in mTuba-stimulated ruffling, we exposed serum-starved B16 cells to wortmannin, but the formation of mTuba puncta and ruffling were not inhibited within 30 minutes of treatment (Table 2).

It should be noted that PtdIns(4,5)P_2 is also a product of the action of phosphatidylinositol 4-phosphate 5-kinase type Iα (PIP5Kα), which is regulated by Rho-family GTPases (Chong et al., 1994; Doughman et al., 2003; Oude Weernink et al., 2004) and Arf-family GTPases (Honda et al., 1999; Wong and Isberg, 2003). Overexpression of PIP5Kα increases cellular concentrations of PtdIns(4,5)P_2 and drives actin polymerization at these lipid microdomains (Rozelle et al., 2000), and N-WASP has been shown to be a crucial component for actin polymerization in the comet tails of rocketing PtdIns(4,5)P_2 vesicles (Benesch et al., 2005). PIP5Kα overexpression stimulated the formation of rocketing vesicles in B16 cells, often with long actin tails (Fig. 6B). mTuba was visualized in the comet tail, but concentrated at the head of vesicles (Figs 6A,B). Since, mTuba is incapable of binding dynamin, and as dynamin function has been shown to be important for the regulation of comet tail length of PIP5Kα-generated vesicles (Orth et al., 2002), the unusual length of the induced actin comets might reflect the inability of this Tuba isoform to recruit dynamin to the vesicle. The presence of N-

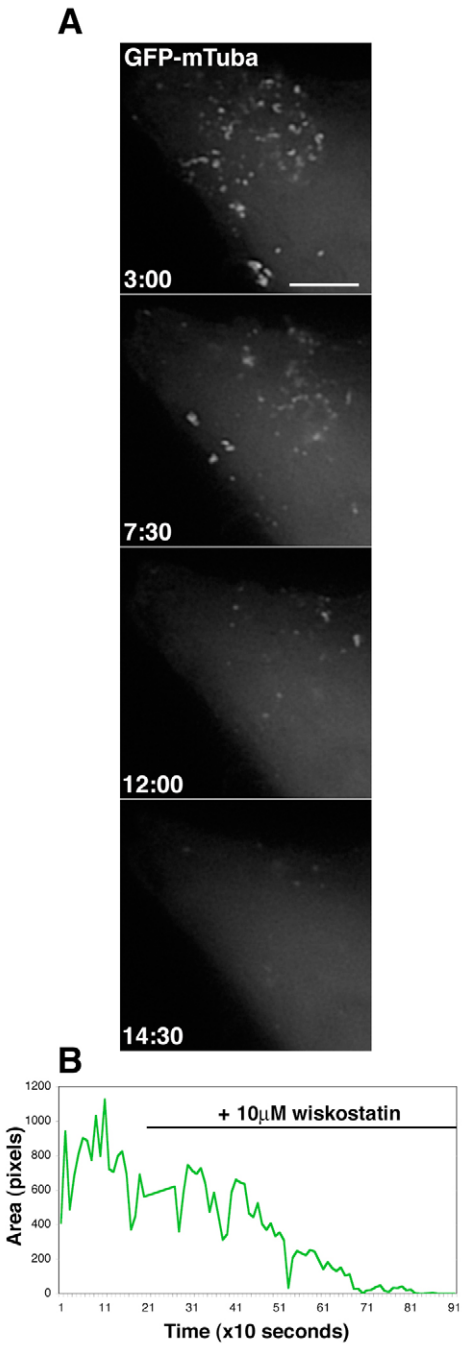

Fig. 5. N-WASP activity is essential for mTuba ruffling. (A) B16 cells were transfected with GFP-mTuba and treated with 10 μM wiskostatin. Images depict mTuba puncta following addition of drug. Wiskostatin abolishes dorsal ruffling and disperses mTuba puncta. (B) Graphical representation of the time-lapse movie from A. Images were thresholded to include the puncta, and the number of thresholded pixels were plotted as a function of time. The intensity of mTuba puncta is reduced by 50% after five minutes treatment and has completely dispersed 8 minutes after addition of the drug (n=3). Bar, 10 μm.

WASP at PIP5Kα-induced vesicles was also confirmed (data not shown).

To examine the role of Tuba in comet tail formation, two RNAi constructs were designed to knockdown expression of both Tuba isoforms and were directed to a region between the GEF and BAR domains ('A'), and a region between the two C-terminal SH3 domains ('B', Fig. 6C). 72 hours post-transfection, ~75% knockdown of Tuba and mTuba was observed in B16 cells (Fig. 6D) and these constructs were observed to restrict or inhibit dorsal ruffling ('A' and 'B' respectively, Table 2). RNAi knockdown of Tuba with either RNAi construct decreased the number of comets formed per cell (PIP5K+RNAi 'A': average=1.4 comets/cell, n=26; PIP5K+RNAi 'B': average=1.1 comets/cell, n=27) when compared with B16 cells transfected with PIP5Kα alone (Fig. 6E; PIP5Kα: average=3.3 comets/cell, n=18), with a significant decrease observed for RNAi 'B'. Additionally, co-expression of mTuba with PIP5Kα increased the number of comet tails observed per cell significantly (PIP5K+mTuba: average=6.1 comets/cell, n=28) relative to PIP5Kα-transfected cells. This suggests that Tuba might have a role in the regulation of N-WASP-dependent vesicle rocketing. Together with the data from dorsal ruffling, these results suggest that N-WASP and mTuba associate during multiple actin-dependent processes, and that these proteins might link actin polymerization to sensing of PtdIns(4,5)P_2-rich domains.

Invasion of B16 cells towards fibronectin is reduced by RNAi knockdown of Tuba isoforms

Cellular invasion entails a complex interplay of events from adhesion, to motility and matrix degradation. In all cases, the establishment of a spatially restricted platform for actin assembly is required to polarize the membrane and initiate movement. N-WASP is observed at cell protrusions considered precursors to cell movement such as podosomes (Osiak et al., 2005), invadopodia (Golub and Caroni, 2005; Yamaguchi et al., 2005) and lamellipodia (Golub and Caroni, 2005). As the core components of N-WASP-dependent actin assembly were observed to localize to puncta at mTuba-induced membrane ruffles, we hypothesized that Tuba might have a functional role in invasion. Serum-starved B16 cells cultured on top of a Matrigel plug in serum-free medium will invade the underlying gel towards a fibronectin cue (Kobayashi et al., 1992). To examine the role of Tuba in invasion, B16 cells were transfected with RNAi 'A', or RNAi 'B' (Fig. 6C), or a control GFP construct. 48 hours post-transfection, serum-starved cells were FACS sorted for identical expression levels and seeded onto Matrigel plugs for 22 hours. Control GFP-transfected

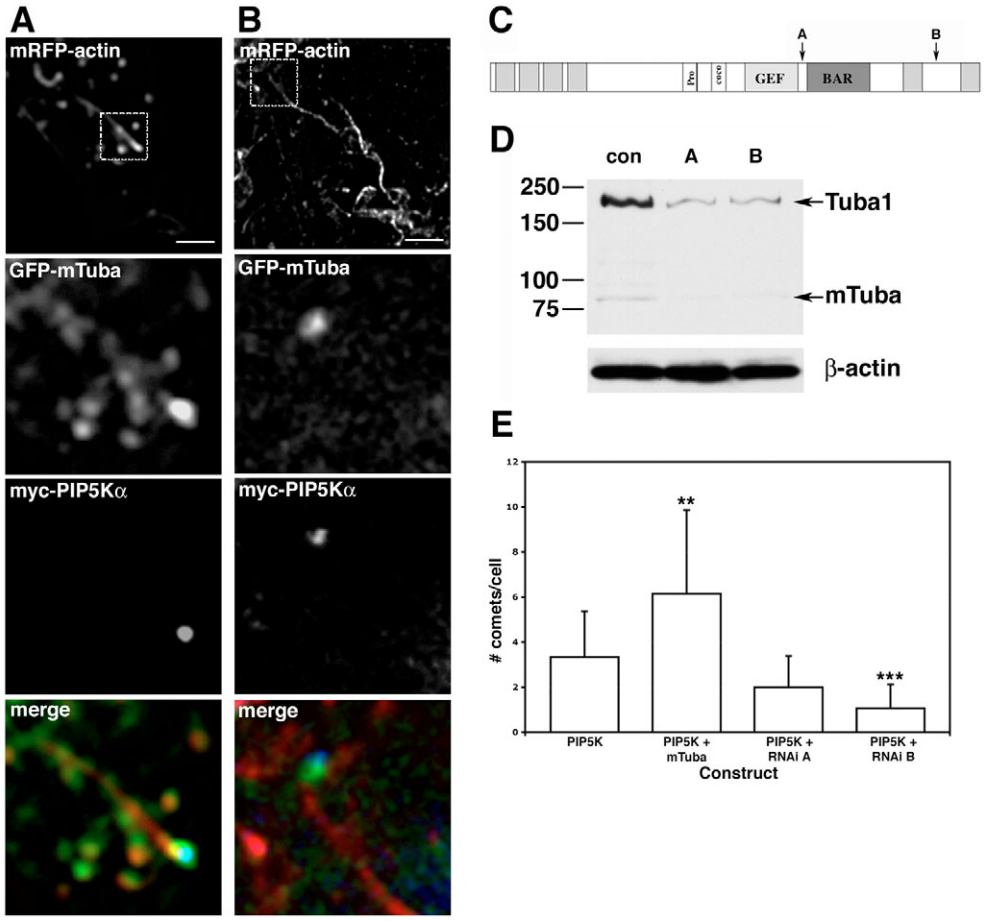

Fig. 6. B16 cells were co-transfected with myc-PIP5Kα, GFP-mTuba and mRFP-actin. Cells were cultured on glass coverslips and fixed. (A) GFP-mTuba incorporates into comet tails and concentrates at the vesicles. Box indicates region examined in lower panels. (B) PIP5Kα expression often generated long-tailed comets with mTuba concentrated at the vesicle. Box indicates region examined in lower panels. (C) Schematic representation of targeted sites for RNAi. 'A' targets a region in Tuba between the GEF and BAR domains. 'B' targets a region between the two C-terminal SH3 domains. (D) B16 cells transfected with control plasmid, RNAi 'A' or RNAi 'B' were FACS sorted for equivalent expression (50% intensity and above) at 48 hours and lysed 72 hours post-transfection. Cell lysates were subjected to SDS-PAGE and probed with Tuba antibody (Tuba #5415) and β-actin antibody (loading control). Both RNAi constructs resulted in ~75% knockdown of both Tuba and mTuba. (E) B16 cells were transfected with either pRK5myc-PIP5Kα alone (PIP5K), pRK5myc-PIP5Kα and Cherry-mTuba (PIP5K + mTuba), pRK5myc-PIP5Kα and RNAi 'A' (PIP5K + RNAi A), or pRK5myc-PIP5Kα and RNAi 'B' (PIP5K + RNAi B). Cells were cultured on glass coverslips and fixed. The number of comets formed per cell was quantitated. RNAi 'B' significantly reduced the number of comets observed per cell relative to cells transfected with PIP5Kα alone. Error bars represent s.d. (***P<0.005, **P<0.01). Bars: A,B, 5 μm.

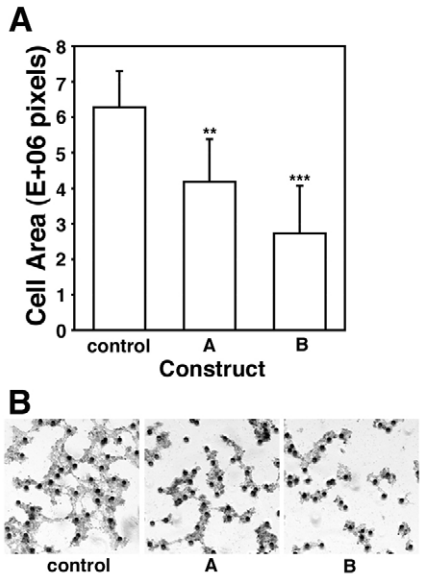

Fig. 7. Tuba RNAi knockdown inhibits invasive behavior of B16 cells. (A) Matrigel invasion assays of B16 cells transfected with the indicated vectors. Error bars represent s.d. (***P<0.005, **P<0.01). (B) Representative images of the PET membranes from the bottom of Matrigel invasion chambers. Cell area was calculated using Metamorph software and corrected for pore area (see Materials and Methods).

cells invade Matrigel and pass through 8 μm pores to the fibronectin-coated underside of a PET membrane (Fig. 7B). By contrast, cells transfected with Tuba RNAi constructs demonstrated impairment of the invasive phenotype (Fig. 7A,B), with expression of RNAi 'B' reducing the ability of cells to invade by greater than 50% (n=6). Therefore, Tuba is required for efficient invasion of B16 cells. Interestingly, knockdown of Tuba with either RNAi 'A' or RNAi 'B' did not inhibit circumferential ruffling in serum-starved B16 cells (data not shown).

Discussion

The domain structure of Tuba suggests its potential to act as a scaffold for the recruitment, coordination and regulation of signaling molecules and molecular machinery involved in membrane-proximal cellular events. Overexpression of mTuba, an isoform of Tuba lacking the dynamin-binding SH3 domains, induced uncoordinated dorsal ruffling, distinct from conventional circular dorsal waves, in the low metastatic B16-F1 cell line. The ability of mTuba to stimulate ruffling suggests that dynamin is not required for this process. However, as Tuba 1 was observed to co-localize with mTuba at puncta when co-expressed (Table 1), we cannot rule out the possibility that dynamin function is integrated through the dimerization of different Tuba isoforms.

Interaction with actin-regulatory proteins was shown to be a key determinant for mTuba-stimulated membrane ruffling as deletion of the C-terminal SH3 domain prevented puncta and ruffle formation. Moreover, specific inhibition of N-WASP using a small molecule inhibitor collapsed mTuba-based puncta. Thus, N-WASP activity is essential for the recruitment and function of mTuba in dorsal ruffles.

Core components of N-WASP-stimulated actin assembly were shown to associate with mTuba puncta. Perturbed ruffling and an overproduction of puncta were observed following co-expression of dominant-negative Cdc42, consistent with a nucleotide switch controlling the affinity of Cdc42 for N-WASP; indeed, it appears that a saturated Cdc42-GTP–N-WASP complex has greater affinity for Arp2/3 (Leung and Rosen, 2005). Additionally, mTuba GEF activity was required for productive ruffling consistent with a requirement for the activation of N-WASP by this GTPase (Kim et al., 2000; Miki et al., 1998).

It has been proposed that N-WASP activation is a two-step process that involves the interaction of Cdc42 with Toca-1, with subsequent binding of N-WASP (Ho et al., 2004). Interestingly, we observed localization of Toca-1 to mTuba puncta. Bovine brain extracts immunodepleted of Toca-1 were unable to support PtdIns(4,5)P_2 activation of N-WASP, and it was proposed that PtdIns(4,5)P_2 might regulate N-WASP activity through juxtapositioning of a regulator, such as a GEF (Ho et al., 2004). PtdIns(4,5)P_2 is primarily localized in the plasma membrane where it acts as a marker for actin assembly (Balla and Varnai, 2002; Huang et al., 2004; Meyer and Teruel, 2003), and recently it was demonstrated that N-WASP activation is ultrasensitive to small increases in PtdIns(4,5)P_2 density (Papayannopoulos et al., 2005). FRET analysis has described positioning of active N-WASP at membrane protrusions (Lorenz et al., 2004) and together these results suggest that N-WASP might function in mTuba-directed actin assembly through acute sensing of local membrane domains, marking a site for localized activation of Cdc42 by mTuba and subsequent regulation of Arp2/3 activity. Of note, deletion of the BAR domain prevented the localization of mTuba to puncta in dorsal ruffles. BAR domains do not exhibit strong lipid specificity (Peter et al., 2004); therefore, it is plausible that recruitment of mTuba to cytoskeletal structures through direct interaction with N-WASP confers lipid specificity to the BAR domain by increasing its proximity to PtdIns(4,5)P_2-containing lipid microdomains.

We additionally observed localization of WIP at mTuba-induced ruffles. WIP has been shown to negatively regulate Cdc42–N-WASP-stimulated Arp2/3 activity (Martinez-Quiles et al., 2001). However, WIP is required for N-WASP-dependent actin-based motility of vaccinia (Moreau et al., 2000), and interaction of WIP with cortactin has been proposed to positively regulate actin assembly at the cell periphery (Kinley et al., 2003). Since cortactin was observed to localize to a subpopulation of mTuba puncta, it is possible that a WIP-cortactin complex regulates mTuba puncta. However, cortactin localization was not as robust as that of N-WASP, WIP or Toca-1, suggesting that a cortactin-WIP interaction is not crucial for mTuba function. Activation of an N-WASP–WIP complex by Cdc42 has been shown to require the presence of Toca-1 (Ho et al., 2004); therefore, it is more likely that mTuba-stimulated, N-WASP-dependent actin assembly involves a complex interplay of Toca-1 and WIP for control.

Overexpression of PIP5Kα stimulated PtdIns(4,5)P_2 vesicle formation in mTuba-transfected B16 cells and mTuba was observed to localize to PIP5Kα-induced actin comets coincident with N-WASP, PIP5Kα and actin. A requirement of N-WASP for vesicle rocketing (Benesch et al., 2002) combined with the localization of mTuba at PIP5Kα-induced vesicles suggests that mTuba-stimulated ruffling through the N-WASP

microdomain sensing occurs downstream of PIP5Kα activity, which is also observed for Arf-6 stimulation of membrane ruffling (Honda et al., 1999). The observed reduction in comet tail formation with Tuba knockdown implicates Tuba in the regulation of comet tail formation through the establishment of a membrane-proximal protein scaffold. Of note, the observed generation of rocketing vesicles with long actin tails might reflect the inability of this Tuba isoform to bind and recruit dynamin to vesicles for the regulation of actin dynamics and comet tail length (Orth et al., 2002), and might represent an isoform-specific difference in N-WASP-dependent actin assembly.

In this study, we have described a mechanism of mTuba membrane protrusion that is N-WASP dependent. N-WASP activity is required for the formation of invadopodia (Yamaguchi et al., 2005) and localizes to podosomes (Osiak et al., 2005), membrane structures that are required for cellular matrix degradation and invasion. Additionally, N-WASP activity has been shown to be required for hepatocyte growth factor (HGF)-induced invasion (Yamaguchi et al., 2002). RNAi knockdown of Tuba retarded cellular invasion. As Tuba isoforms are involved in multiple cellular events in addition to membrane ruffling, it is difficult to establish a definitive inhibitory action of Tuba on the invasive behavior of B16 cells. However, both Tuba isoforms are observed to localize to puncta in ruffles (Table 1), and RNAi knockdown obliterated dorsal ruffling (Table 2) without affecting circumferential ruffling. Combined, these results establish Tuba function in dorsal ruffling as significant for cellular invasion, and mTuba-stimulated dorsal ruffling might represent an as-yet-unidentified mechanism for the control of N-WASP-activated actin assembly during cell migration and invasion.

Analysis of the function of individual Tuba isoforms is complicated by the innate ability of these isoforms to interact through heterodimerization. We propose that interaction of mTuba with N-WASP results in recruitment of this complex to the plasma membrane through lipid microdomain sensing and is associated with concomitant activation of N-WASP through direct interaction of Cdc42-GTP and PtdIns(4,5)P_2. Subsequent Arp2/3 activation stimulates actin assembly and membrane protrusion, which is regulated through the transient interaction of N-WASP accessory proteins including cortactin, WIP, Toca-1 and dynamin. Through these interactions, subpopulations of Tuba might integrate different cellular functions, including dorsal ruffling and endocytosis, to facilitate crucial cellular processes such as invasion.

Materials and Methods

DNA constructs

Subcloning and PCR were performed using standard methods. GFP-mTuba (2598 bp) was constructed by amplification of region 2130-4728 of EST clone (IMAGE 4329464; Invitrogen), which was subsequently cloned into the *Hin*dIII and *Bam*HI sites of EGFP-C1 (Clontech). Cherry-mTuba was constructed by specific amplification of the Cherry fluorophore from mCherry, a kind gift of R. Tsien (HHMI, San Diego, CA) (Shaner et al., 2004), and used to replace the GFP fluorophore in EGFP-mTuba (Cherry-mTuba).

Tuba-knockdown constructs were made by cloning Tuba-specific oligonucleotides (mouse Tuba, 'A': forward, 5′-TgaagatagcctgatggaaaTTCAAGAGAtttccatcaggctatcttcTTTTTTC-3′; reverse, 5′-TCGAGAAAAAAgaagatagcctgatggaaaTCTCTTGAAtttccatcaggctatcttca-3′; mouse Tuba, 'B': forward, 5′-Tggacaacggagtcaccaaa TTCAAGAGAtttggtgactccgttgtccTTTTTC-3′; reverse, 5′-tcgagAAAAAAggacaacggagtcaccaaaTCTCTTGAAtttggtgactccgttgtccA-3′) into pLL3.7 as described (Rubinson et al., 2003). Constructs were designed in accordance with published recommendations (Reynolds et al., 2004) and were verified by DNA sequencing. GFP-Arp3 was constructed by M. Welch (Welch et al., 1997). pRK5myc-PIP5KIα, pRK5myc-wtCdc42, pRK5myc-N17Cdc42 and pRK5myc-N17Rac were kind gifts of L. Machesky (University of Birmingham, Birmingham, UK). The GTPase from pRK5myc-wtCdc42 was amplified and subcloned into pEGFP-C1 (GFP-Cdc42). pcDNA3-GFP-WIP was a kind gift of N. Ramesh (Harvard Medical School, MA). mRFP-β-actin was a kind gift of S. Halpain (The Scripps Research Institute, CA). GFP-Toca-1 was a kind gift of P. De Camilli (HHMI, Yale, CT).

Protein and antibody production

A fragment encoding the final 292 amino acids of human Tuba (Tuba-GST-292) was generated by PCR (KIAA1010 clone; Kazusa DNA Research Institute) and cloned into the pGEX-6P-1 vector (Amersham Pharmacia Biotech). The protein was purified according to the manufacturer's recommendations and immobilized on glutathione sepharose. Immobilized Tuba-GST-292 was digested with PreScission™ protease to remove the GST tag (Amersham Pharmacia Biotech) and the purified Tuba protein was used to raise polyclonal rabbit antiserum #5415 (Covance).

Cell culture and fluorescence microscopy

B16-F1 (ATCC CRL-6323) cells were cultured as recommended by ATCC. Cell transfections were performed using Amaxa technology with cell nucleofection solution R, and program D-09 according to the manufacturer's recommendations (http://www.Amaxa.org). Transfected cells were incubated for 15-20 hours at 37°C before further experimentation. For immunofluorescence analysis, cells were plated on acid-washed coverslips. Cells were fixed with 4% (w/v) paraformaldehyde (PFA) in PGKS [145 mM NaCl, 5 mM KCl, 1.2 mM $CaCl_2$, 1.3 mM $MgCl_2$, 1.2 mM NaH_2PO_4, 20 mM HEPES, 10 mM glucose, 400 mM sucrose, 4% (w/v) PFA, pH 7.3)] for 25 minutes at room temperature and permeabilized with 0.25% (v/v) Triton X-100 in PBS. Antibodies used were affinity-purified (defined as 'AP' in the text and figures) anti-Tuba polyclonal antibody (pAb), anti-Tuba pAb #5415 (Salazar et al., 2003), anti-N-WASP pAb (Rohatgi et al., 1999), anti-β-actin monoclonal antibody (mAb) AC15 (Sigma, A-5441), anti-GFP pAb AV (BD Biosciences, 8372-1), anti-cortactin mAb 4F11 (Upstate, 05-180), anti-GM130 mAb (BD Biosciences, 610823), anti-caveolin pAb (Transduction Labs, 610059), anti-dynamin mAb (Upstate, 05-330), Texas-Red-conjugated transferrin (Molecular Probes, T-02875), lysine-fixable Texas-Red-conjugated dextran 70,000 M_r (Molecular Probes, D-1864), anti-myc mAb 9E10 (Santa Cruz, sc-40). Images were collected on a Deltavision system (Applied Precision) and processed using Photoshop 7.0 (Adobe). For live cell imaging, each fluorophore was exposed once every 10 seconds for a total duration of 10-15 minutes.

Quantitation of co-localization

Co-localization of fluorescence overlap at puncta was calculated using Metamorph software (Universal Imaging Corporation). Puncta were enhanced as previously described (Kabir et al., 2001). Briefly, fluorescent images were processed sequentially with the following filters: unsharp mask, low pass, laplace edge detection, low pass. The background corrected images were thresholded and the measurement of co-localization function used to calculate the amount of overlap of each of the fluorophores for every frame in a movie (Movie 1, supplementary material). The resultant numbers were plotted as a measure of percentage of overlap with ruffle progression.

Drug treatment

Cytochalasin D treatment and kymography were performed as described previously (Bear et al., 2002). Serum-starved mTuba-expressing cells were treated with 60 nM wortmannin (Sigma, W-1628) or DMSO control for 30 minutes. Similarly, mTuba-expressing cells were exposed to 10 μM wiskostatin (Calbiochem, 681525) for 10-15 minutes. To observe transferrin uptake, cells were incubated on ice for 30 minutes in the presence of 25 μg/ml Texas-Red–transferrin, washed once, then incubated at 37°C for 20 minutes before being fixed with 4% PFA. Fluorescent dextran uptake was performed as described previously (Turvey and Thorn, 2004).

Western blot analysis

Cells were lysed with ice-cold GST buffer [50 mM Tris-HCl, 200 mM NaCl, 1% (v/v) IGEPAL CA-630, 2 mM $MgCl_2$, 10% (v/v) glycerol, pH 7.4)], phosphatase inhibitors (1 mM Na_3VO_4, 10 mM NaF), and a protease inhibitor cocktail (Roche complete protease inhibitor tablets without EDTA). Lysates were incubated for 30 minutes on ice and centrifuged for 15 minutes at 18,000 ***g***, 4°C. Protein concentrations were quantitated using the BCA Assay Kit (Pierce) according to the manufacturer's recommendations, and separated on 7.5% SDS-PAGE gels and transferred to Immobilon-P membranes (Millipore). Membranes were probed with primary antibodies and HRP-coupled donkey anti-mouse and/or anti-rabbit secondary antibodies (Jackson Immunologicals) and developed using the ECL Plus kit (Amersham-Pharmacia Biotech).

Invasion assays

B16-F1 cells were Amaxa transfected and sorted by fluorescence-activated cell

sorting (FACS) for 50% or higher EGFP expression 48 hours following transfection and used immediately. Tumor cell invasiveness was determined as described previously (Kurisu et al., 2005) with modifications. Briefly, a layer of Phenol-Red-free Matrigel (#356237, BD Biosciences) was added to the inner chamber of a 24-well PET 8 μm cell culture insert (Falcon 35-3097) and solidified at 37°C for 2 hours. The underside of the membranes were coated with 25 μg/ml fibronectin (F-1141; Sigma) at room temperature for 1 hour, followed by three washes with MEM+0.35% BSA. 1 ml of MEM+0.35% BSA was added to the lower chamber and 2.5×10^4 cells in MEM+0.35% BSA were added to each insert and incubated for 22 hours at 37°C. The Matrigel was removed from the inner chamber with a cotton swab and the membranes were fixed with 4% PFA. Cells that had migrated to the underside of the membrane were stained with 0.4% Crystal Violet and washed extensively. Phase contrast images were taken with a Nikon TE300 fitted with a SpotFLEX CCD camera (FX1520, SciTech). Nine random fields were taken for each membrane and the number of cells that had migrated to the lower surface was quantitated using Metamorph software. Briefly, the area of the membrane occupied by cellular material was calculated by applying the Integrated Morphology function to thresholded images. Values for each membrane were corrected for pore area.

We thank R. Tsien (HHMI, San Diego, CA) and M. Welch (University of California, Berkley, CA) for the mCherry and GFP-Arp3 constructs, respectively, as well as L. Machesky (University of Birmingham, Birmingham, UK) for the pRK5-mycPIP5KIα and pRK5myc-wtCdc42 constructs, N. Ramesh (Harvard Medical School, MA) for pcDNA3-GFP-WIP, S. Halpain (The Scripps Research Institute, CA) for mRFP-β-actin and P. De Camilli (HHMI, Yale, CT) for GFP-Toca-1. We thank A. Kwiatkowski for mRFP-Evl and Tuba reagents. K. O'Brien is greatly acknowledged for her technical assistance. We thank M. Barzik, E. Dent and C. Furman for critically reading the manuscript. Many thanks to E. Dent for sharing his knowledge of microscopy. F.B.G. is supported by NIH grant GM58801. R.S.M. is supported by NCI training grant T32-CA09216E-25.

References

Balla, T. and Varnai, P. (2002). Visualizing cellular phosphoinositide pools with GFP-fused protein-modules. *Sci. STKE* **2002**, PL3.

Bear, J. E., Loureiro, J. J., Libova, I., Fassler, R., Wehland, J. and Gertler, F. B. (2000). Negative regulation of fibroblast motility by Ena/VASP proteins. *Cell* **101**, 717-728.

Bear, J. E., Svitkina, T. M., Krause, M., Schafer, D. A., Loureiro, J. J., Strasser, G. A., Maly, I. V., Chaga, O. Y., Cooper, J. A., Borisy, G. G. et al. (2002). Antagonism between Ena/VASP proteins and actin filament capping regulates fibroblast motility. *Cell* **109**, 509-521.

Benesch, S., Lommel, S., Steffen, A., Stradal, T. E., Scaplehorn, N., Way, M., Wehland, J. and Rottner, K. (2002). Phosphatidylinositol 4,5-biphosphate (PIP2)-induced vesicle movement depends on N-WASP and involves Nck, WIP, and Grb2. *J. Biol. Chem.* **277**, 37771-37776.

Benesch, S., Polo, S., Lai, F. P., Anderson, K. I., Stradal, T. E., Wehland, J. and Rottner, K. (2005). N-WASP deficiency impairs EGF internalization and actin assembly at clathrin-coated pits. *J. Cell Sci.* **118**, 3103-3115.

Carlier, M. F., Nioche, P., Broutin-L'Hermite, I., Boujemaa, R., Le Clainche, C., Egile, C., Garbay, C., Ducruix, A., Sansonetti, P. and Pantaloni, D. (2000). GRB2 links signaling to actin assembly by enhancing interaction of neural Wiskott-Aldrich syndrome protein (N-WASp) with actin-related protein (ARP2/3) complex. *J. Biol. Chem.* **275**, 21946-21952.

Chong, L. D., Traynor-Kaplan, A., Bokoch, G. M. and Schwartz, M. A. (1994). The small GTP-binding protein Rho regulates a phosphatidylinositol 4-phosphate 5-kinase in mammalian cells. *Cell* **79**, 507-513.

Cooper, J. A. (1987). Effects of cytochalasin and phalloidin on actin. *J. Cell Biol.* **105**, 1473-1478.

Doughman, R. L., Firestone, A. J., Wojtasiak, M. L., Bunce, M. W. and Anderson, R. A. (2003). Membrane ruffling requires coordination between type Ialpha phosphatidylinositol phosphate kinase and Rac signaling. *J. Biol. Chem.* **278**, 23036-23045.

Dowrick, P., Kenworthy, P., McCann, B. and Warn, R. (1993). Circular ruffle formation and closure lead to macropinocytosis in hepatocyte growth factor/scatter factor-treated cells. *Eur. J. Cell Biol.* **61**, 44-53.

Farsad, K., Ringstad, N., Takei, K., Floyd, S. R., Rose, K. and De Camilli, P. (2001). Generation of high curvature membranes mediated by direct endophilin bilayer interactions. *J. Cell Biol.* **155**, 193-200.

Fukuoka, M., Suetsugu, S., Miki, H., Fukami, K., Endo, T. and Takenawa, T. (2001). A novel neural Wiskott-Aldrich syndrome protein (N-WASP) binding protein, WISH, induces Arp2/3 complex activation independent of Cdc42. *J. Cell Biol.* **152**, 471-482.

Golub, T. and Caroni, P. (2005). PI(4,5)P2-dependent microdomain assemblies capture microtubules to promote and control leading edge motility. *J. Cell Biol.* **169**, 151-165.

Higgs, H. N. and Pollard, T. D. (2000). Activation by Cdc42 and PIP(2) of Wiskott-Aldrich syndrome protein (WASp) stimulates actin nucleation by Arp2/3 complex. *J. Cell Biol.* **150**, 1311-1320.

Higgs, H. N. and Pollard, T. D. (2001). Regulation of actin filament network formation through ARP2/3 complex: activation by a diverse array of proteins. *Annu. Rev. Biochem.* **70**, 649-676.

Ho, H. Y., Rohatgi, R., Lebensohn, A. M., Le, M., Li, J., Gygi, S. P. and Kirschner, M. W. (2004). Toca-1 mediates Cdc42-dependent actin nucleation by activating the N-WASP-WIP complex. *Cell* **118**, 203-216.

Honda, A., Nogami, M., Yokozeki, T., Yamazaki, M., Nakamura, H., Watanabe, H., Kawamoto, K., Nakayama, K., Morris, A. J., Frohman, M. A. et al. (1999). Phosphatidylinositol 4-phosphate 5-kinase alpha is a downstream effector of the small G protein ARF6 in membrane ruffle formation. *Cell* **99**, 521-532.

Huang, S., Lifshitz, L., Patki-Kamath, V., Tuft, R., Fogarty, K. and Czech, M. P. (2004). Phosphatidylinositol-4,5-bisphosphate-rich plasma membrane patches organize active zones of endocytosis and ruffling in cultured adipocytes. *Mol. Cell. Biol.* **24**, 9102-9123.

Jiang, W. G. (1995). Membrane ruffling of cancer cells: a parameter of tumour cell motility and invasion. *Eur. J. Surg. Oncol.* **21**, 307-309.

Kabir, N., Schaefer, A. W., Nakhost, A., Sossin, W. S. and Forscher, P. (2001). Protein kinase C activation promotes microtubule advance in neuronal growth cones by increasing average microtubule growth lifetimes. *J. Cell Biol.* **152**, 1033-1044.

Kempiak, S. J., Yamaguchi, H., Sarmiento, C., Sidani, M., Ghosh, M., Eddy, R. J., Desmarais, V., Way, M., Condeelis, J. and Segall, J. E. (2005). A neural Wiskott-Aldrich Syndrome protein-mediated pathway for localized activation of actin polymerization that is regulated by cortactin. *J. Biol. Chem.* **280**, 5836-5842.

Kessels, M. M. and Qualmann, B. (2002). Syndapins integrate N-WASP in receptor-mediated endocytosis. *EMBO J.* **21**, 6083-6094.

Kim, A. S., Kakalis, L. T., Abdul-Manan, N., Liu, G. A. and Rosen, M. K. (2000). Autoinhibition and activation mechanisms of the Wiskott-Aldrich syndrome protein. *Nature* **404**, 151-158.

Kinley, A. W., Weed, S. A., Weaver, A. M., Karginov, A. V., Bissonette, E., Cooper, J. A. and Parsons, J. T. (2003). Cortactin interacts with WIP in regulating Arp2/3 activation and membrane protrusion. *Curr. Biol.* **13**, 384-393.

Kisseleva, M., Feng, Y., Ward, M., Song, C., Anderson, R. A. and Longmore, G. D. (2005). The LIM protein Ajuba regulates phosphatidylinositol 4,5-bisphosphate levels in migrating cells through an interaction with and activation of PIPKI alpha. *Mol. Cell. Biol.* **25**, 3956-3966.

Kobayashi, H., Ohi, H., Sugimura, M., Shinohara, H., Fujii, T. and Terao, T. (1992). Inhibition of in vitro ovarian cancer cell invasion by modulation of urokinase-type plasminogen activator and cathepsin B. *Cancer Res.* **52**, 3610-3614.

Kurisu, S., Suetsugu, S., Yamazaki, D., Yamaguchi, H. and Takenawa, T. (2005). Rac-WAVE2 signaling is involved in the invasive and metastatic phenotypes of murine melanoma cells. *Oncogene* **24**, 1309-1319.

Leung, D. W. and Rosen, M. K. (2005). The nucleotide switch in Cdc42 modulates coupling between the GTPase-binding and allosteric equilibria of Wiskott-Aldrich syndrome protein. *Proc. Natl. Acad. Sci. USA* **102**, 5685-5690.

Lorenz, M., Yamaguchi, H., Wang, Y., Singer, R. H. and Condeelis, J. (2004). Imaging sites of N-wasp activity in lamellipodia and invadopodia of carcinoma cells. *Curr. Biol.* **14**, 697-703.

Machesky, L. M. and Insall, R. H. (1998). Scar1 and the related Wiskott-Aldrich syndrome protein, WASP, regulate the actin cytoskeleton through the Arp2/3 complex. *Curr. Biol.* **8**, 1347-1356.

Martinez-Quiles, N., Rohatgi, R., Anton, I. M., Medina, M., Saville, S. P., Miki, H., Yamaguchi, H., Takenawa, T., Hartwig, J. H., Geha, R. S. et al. (2001). WIP regulates N-WASP-mediated actin polymerization and filopodium formation. *Nat. Cell Biol.* **3**, 484-491.

Mellstrom, K., Heldin, C. H. and Westermark, B. (1988). Induction of circular membrane ruffling on human fibroblasts by platelet-derived growth factor. *Exp. Cell Res.* **177**, 347-359.

Meyer, T. and Teruel, M. N. (2003). Fluorescence imaging of signaling networks. *Trends Cell Biol.* **13**, 101-106.

Miki, H., Sasaki, T., Takai, Y. and Takenawa, T. (1998). Induction of filopodium formation by a WASP-related actin-depolymerizing protein N-WASP. *Nature* **391**, 93-96.

Moreau, V., Frischknecht, F., Reckmann, I., Vincentelli, R., Rabut, G., Stewart, D. and Way, M. (2000). A complex of N-WASP and WIP integrates signalling cascades that lead to actin polymerization. *Nat. Cell Biol.* **2**, 441-448.

Orth, J. D., Krueger, E. W., Cao, H. and McNiven, M. A. (2002). The large GTPase dynamin regulates actin comet formation and movement in living cells. *Proc. Natl. Acad. Sci. USA* **99**, 167-172.

Osiak, A. E., Zenner, G. and Linder, S. (2005). Subconfluent endothelial cells form podosomes downstream of cytokine and RhoGTPase signaling. *Exp. Cell Res.* **307**, 342-353.

Oude Weernink, P. A., Schmidt, M. and Jakobs, K. H. (2004). Regulation and cellular roles of phosphoinositide 5-kinases. *Eur. J. Pharmacol.* **500**, 87-99.

Papayannopoulos, V., Co, C., Prehoda, K. E., Snapper, S., Taunton, J. and Lim, W. A. (2005). A polybasic motif allows N-WASP to act as a sensor of PIP(2) density. *Mol. Cell* **17**, 181-191.

Peter, B. J., Kent, H. M., Mills, I. G., Vallis, Y., Butler, P. J., Evans, P. R. and McMahon, H. T. (2004). BAR domains as sensors of membrane curvature: the amphiphysin BAR structure. *Science* **303**, 495-499.

Peterson, J. R., Bickford, L. C., Morgan, D., Kim, A. S., Ouerfelli, O., Kirschner, M.

W. and Rosen, M. K. (2004). Chemical inhibition of N-WASP by stabilization of a native autoinhibited conformation. *Nat. Struct. Mol. Biol.* **11**, 747-755.

Prehoda, K. E., Scott, J. A., Mullins, R. D. and Lim, W. A. (2000). Integration of multiple signals through cooperative regulation of the N-WASP-Arp2/3 complex. *Science* **290**, 801-806.

Raucher, D., Stauffer, T., Chen, W., Shen, K., Guo, S., York, J. D., Sheetz, M. P. and Meyer, T. (2000). Phosphatidylinositol 4,5-bisphosphate functions as a second messenger that regulates cytoskeleton-plasma membrane adhesion. *Cell* **100**, 221-228.

Reynolds, A., Leake, D., Boese, Q., Scaringe, S., Marshall, W. S. and Khvorova, A. (2004). Rational siRNA design for RNA interference. *Nat. Biotechnol.* **22**, 326-330.

Rohatgi, R., Ma, L., Miki, H., Lopez, M., Kirchhausen, T., Takenawa, T. and Kirschner, M. W. (1999). The interaction between N-WASP and the Arp2/3 complex links Cdc42-dependent signals to actin assembly. *Cell* **97**, 221-231.

Rohatgi, R., Ho, H. Y. and Kirschner, M. W. (2000). Mechanism of N-WASP activation by CDC42 and phosphatidylinositol **4**, 5-bisphosphate. *J. Cell Biol.* **150**, 1299-1310.

Rozelle, A. L., Machesky, L. M., Yamamoto, M., Driessens, M. H., Insall, R. H., Roth, M. G., Luby-Phelps, K., Marriott, G., Hall, A. and Yin, H. L. (2000). Phosphatidylinositol 4,5-bisphosphate induces actin-based movement of raft-enriched vesicles through WASP-Arp2/3. *Curr. Biol.* **10**, 311-320.

Rubinson, D. A., Dillon, C. P., Kwiatkowski, A. V., Sievers, C., Yang, L., Kopinja, J., Rooney, D. L., Ihrig, M. M., McManus, M. T., Gertler, F. B. et al. (2003). A lentivirus-based system to functionally silence genes in primary mammalian cells, stem cells and transgenic mice by RNA interference. *Nat. Genet.* **33**, 401-406.

Salazar, M. A., Kwiatkowski, A. V., Pellegrini, L., Cestra, G., Butler, M. H., Rossman, K. L., Serna, D. M., Sondek, J., Gertler, F. B. and De Camilli, P. (2003). Tuba, a novel protein containing bin/amphiphysin/Rvs and Dbl homology domains, links dynamin to regulation of the actin cytoskeleton. *J. Biol. Chem.* **278**, 49031-49043.

Sampath, P. and Pollard, T. D. (1991). Effects of cytochalasin, phalloidin, and pH on the elongation of actin filaments. *Biochemistry* **30**, 1973-1980.

Shaner, N. C., Campbell, R. E., Steinbach, P. A., Giepmans, B. N., Palmer, A. E. and Tsien, R. Y. (2004). Improved monomeric red, orange and yellow fluorescent proteins derived from Discosoma sp. red fluorescent protein. *Nat. Biotechnol.* **22**, 1567-1572.

Svitkina, T. M. and Borisy, G. G. (1999). Arp2/3 complex and actin depolymerizing factor/cofilin in dendritic organization and treadmilling of actin filament array in lamellipodia. *J. Cell Biol.* **145**, 1009-1026.

Turvey, M. R. and Thorn, P. (2004). Lysine-fixable dye tracing of exocytosis shows F-actin coating is a step that follows granule fusion in pancreatic acinar cells. *Pflugers Arch.* **448**, 552-555.

Weaver, A. M., Heuser, J. E., Karginov, A. V., Lee, W. L., Parsons, J. T. and Cooper, J. A. (2002). Interaction of cortactin and N-WASp with Arp2/3 complex. *Curr. Biol.* **12**, 1270-1278.

Welch, M. D., DePace, A. H., Verma, S., Iwamatsu, A. and Mitchison, T. J. (1997). The human Arp2/3 complex is composed of evolutionarily conserved subunits and is localized to cellular regions of dynamic actin filament assembly. *J. Cell Biol.* **138**, 375-384.

Wong, K. W. and Isberg, R. R. (2003). Arf6 and phosphoinositol-4-phosphate-5-kinase activities permit bypass of the Rac1 requirement for beta1 integrin-mediated bacterial uptake. *J. Exp. Med.* **198**, 603-614.

Yamaguchi, H., Miki, H. and Takenawa, T. (2002). Neural Wiskott-Aldrich syndrome protein is involved in hepatocyte growth factor-induced migration, invasion, and tubulogenesis of epithelial cells. *Cancer Res.* **62**, 2503-2509.

Yamaguchi, H., Lorenz, M., Kempiak, S., Sarmiento, C., Coniglio, S., Symons, M., Segall, J., Eddy, R., Miki, H., Takenawa, T. et al. (2005). Molecular mechanisms of invadopodium formation: the role of the N-WASP-Arp2/3 complex pathway and cofilin. *J. Cell Biol.* **168**, 441-452.

Zalevsky, J., Lempert, L., Kranitz, H. and Mullins, R. D. (2001). Different WASP family proteins stimulate different Arp2/3 complex-dependent actin-nucleating activities. *Curr. Biol.* **11**, 1903-1913.